Circulation Journal
Official Journal of the Japanese Circulation Society
http://www.j-circ.or.jp

ORIGINAL ARTICLE
Imaging

Evaluation of Prosthetic Valve Obstruction on Electrocardiographically Gated Multidetector-Row Computed Tomography

– Identification of Subprosthetic Pannus in the Aortic Position –

Tomohiro Ueda, MD; Hideki Teshima, MD; Shuji Fukunaga, MD;
Shigeaki Aoyagi, MD; Hiroyuki Tanaka, MD

Background: This study was performed to evaluate the diagnostic role of electrocardiographically gated multidetector-row computed tomography (MDCT) for prosthetic valve obstruction (PVO) in the aortic position.

Methods and Results: Between 2002 and 2006, 9 patients were diagnosed with PVO of an aortic bileaflet mechanical valve based on echocardiographic and cineradiographic criteria. These 9 patients were examined using MDCT before replacement of the mechanical valve, and intraoperative findings were compared to morphologic periprosthetic abnormalities observed on MDCT. CT attenuation (Hounsfield units; HU) of the periprosthetic abnormalities was measured to investigate the underlying cause of the PVO. MDCT showed subprosthetic masses extending beyond the prosthetic ring into the orifice of the valve. At reoperation, presence of subprosthetic pannus was confirmed in all of the 9 patients, but no periprosthetic thrombus was found. The mean CT attenuation of the subprosthetic pannus was 170 HU, and it was significantly greater than that obtained from the interventricular septum (108 HU; P<0.0001).

Conclusions: MDCT can be used to clearly visualize subprosthetic pannus causing PVO and the mean CT attenuation of subprosthetic pannus is significantly higher than that of the interventricular septum on MDCT. (*Circ J* 2013; **77:** 418–423)

Key Words: Aortic valve replacement; Cineradiography; Echocardiography; Multidetector-row computed tomography; Prosthetic valve obstruction

Aortic valve replacement (AVR) with a prosthetic cardiac valve is an established therapeutic approach for significant aortic valve disease. Despite recent advances in prosthetic valve technology and anticoagulant therapy, prosthetic valve obstruction (PVO) due to thrombus or pannus is a serious and occasionally fatal valve-related complication.[1–8] The incidence of PVO due to pannus is generally estimated to be 0.1–0.6% per patient-year in the aortic position,[1,2,9] but obstruction of an aortic prosthetic valve caused by pannus is higher in frequency than previously reported and is detected even in asymptomatic patients.[2,4,10] Echocardiography and cineradiography are commonly used diagnostic techniques for PVO,[2,4,11] but identification of the exact cause of PVO, such as thrombus or pannus, is difficult. We have previously reported the usefulness of electrocardiographically (ECG)-gated multidetector-row computed tomography (MDCT) for detecting subprosthetic overgrown pannus in the aortic position in several cases.[12–14]

In this study, we evaluated the role of MDCT in diagnosing PVO and the utility of MDCT in identifying the underlying causes of PVO in the aortic position.

Methods

Patients

The current study was approved by the Ethics Committee of Kurume University, and written informed consent was obtained from all participating patients after they were notified of the risks of radiation exposure and complications due to use of contrast medium.

Received March 27, 2012; revised manuscript received August 26, 2012; accepted September 20, 2012; released online October 19, 2012 Time for primary review: 27 days

Department of Surgery, Kurume University School of Medicine, Kurume (T.U., S.F., H. Tanaka); Department of Cardiovascular Surgery, Chikamori Hospital Heart Center, Kochi (H. Teshima); and Department of Cardiovascular Surgery, Munakata Suikokai General Hospital, Fukutsu (S.A.), Japan

Mailing address: Tomohiro Ueda, MD, Department of Surgery, Kurume University School of Medicine, 67 Asahi-machi, Kurume 830-0011, Japan. E-mail: tomohiro_u17@med.kurume-u.ac.jp

ISSN-1346-9843 doi:10.1253/circj.CJ-12-0290

Table. Patient Clinical Characteristics

Patient no.	Age (years)/ Gender	HR (beats/min)/ Rhythm	Initial operation	Valve size (mm)	Time to MDCT (months)	Velocity index	Opening angle (°)	Cause of PVO at redo surgery	CT attenuation (HU)
1	72/M	62/SR	AVR	SJM 25	100	0.31	23	Pure pannus, Subprosthetic	178
2	62/F	64/SR	DVR	SJM 21	142	0.26	31	Pure pannus, Subprosthetic	178
3	76/F	76/SR	AVR	SJM 21	83	0.41	40	Pure pannus, Subprosthetic	149
4	51/F	68/SR	AVR, Asc Ao Rep	SJM 21	88	0.27	57	Pure pannus, Subprosthetic	166
5	54/F	52/AF	AVR	SJM 25	116	0.28	45	Pure pannus, Subprosthetic	179
6	67/F	72/AF	DVR	SJM 21	139	0.30	30	Pure pannus, Subprosthetic	164
7	71/F	52/AF	AVR	SJM 23	260	0.27	27	Pure pannus, Subprosthetic	165
8	71/F	78/SR	AVR	SJM 23	64	0.48	49	Pure pannus, Subprosthetic	189
9	65/M	76/AF	DVR	SJM 21	153	0.32	43	Pure pannus, Subprosthetic	167

Mean heart rate, 67 beats/min.
AF, atrial fibrillation; Asc Ao Rep, ascending aortic replacement; AVR, aortic valve replacement; CT, computed tomography; DVR, double valve replacement; HR, heart rate; HU, Hounsfield unit; MDCT, multidetector-row computed tomography; PVO, prosthetic valve obstruction; SJM, St. Jude Medical; SR, sinus rhythm.

Among 616 patients who underwent AVR with a St. Jude Medical (SJM) valve (St. Jude Medical, Minneapolis, MN, USA) by the end of 1999, 30 patients (4.9%) underwent replacement of the SJM valve for PVO in the aortic position. Of these 30 patients, 9 (30%) were diagnosed with PVO of the aortic SJM valve on echocardiography and cineradiography and underwent MDCT between 2003 and 2006 to investigate the underlying causes of PVO. The other 21 patients, who underwent replacement of the aortic SJM valve before 2002, were excluded from this study because these patients were diagnosed on echocardiography and cineradiography and MDCT was not available for evaluation of prosthetic valves at our hospital before 2002. These 9 patients received replacement of the SJM valve. The clinical characteristics of these 9 patients are summarized in **Table**, and they form the basis of this study.

Postoperative Anticoagulant Therapy

Anticoagulant therapy consisting of warfarin and an antiplatelet agent (aspirin 100 mg/day) was maintained after AVR, and international normalized ratio (INR) was kept at around 2.0.

Echocardiography and Cineradiography

Transthoracic echocardiography (TTE), including 2-dimensional and Doppler imaging, was performed using a Hewlet-Packard echocardiography system (Yokogawa, USA) and the previously reported technique.[4] Doppler data included peak velocity, peak and mean pressure gradients, effective valve orifice area, and velocity index (VI). Cineradiography was carried out using Siemens-Elema equipment with a C-arm, and the technique previously described was used for measuring leaflet opening and closing angles.[11,15] Opening and closing angles were measured as the distance between the 2 leaflets in the fully open and closed positions. All calculations for Doppler-derived data and measurements of leaflet opening and closing angles were the average of 5 cardiac cycles in patients with atrial fibrillation, and 3 cycles in patients with sinus rhythm or rhythm regulated by a pacemaker. In these 9 patients, there were no subjects with a pacemaker. Based on our previous study,[4] PVO was suspected when VI was <0.35 on TTE and when persistent restriction of leaflet motion was observed on cineradiography with the measured opening angle ≥20°.[2] In this study, PVO was principally diagnosed based on the cineradiographic criteria because previous studies have demonstrated that PVO was detected accurately and far earlier on cineradiography than on TTE.[4,11,14,16]

MDCT

MDCT was performed using a 16-slice Light Speed ULTRA (GE Medical Systems, Yokogawa Medical System, Tokyo, Japan) with ECG-gated half reconstruction in the 9 patients with PVO. In the 16-detector row CT, scanning was based on retrospectively acquired ECG-gated data using a 16×1.25-mm collimation, a scan pitch of 0.4, and a gantry rotation time of 400 ms, and the scanning parameters (120 kVp, 200–700 mA) varied slightly, depending on patient size. No pharmacologic agents were used for the control of heart rate. Patients received 1.2–2.0 ml/kg i.v. non-ionic contrast medium (Iopamiron, 370 mgI/ml; Bayer Holding, Tokyo, Japan) by means of a power injector (Auto Enhance A-50; Nemoto-Kyorin-Dou, Tokyo, Japan) that injected contrast medium at a rate of 3.0 ml/s, and scanning began 45 s after contrast medium was given. Patients were instructed to hold his/her breath, and scanning was initiated and was performed in a craniocaudal direction with simultaneous recording of the ECG trace. The imaging volume was selected from the top of the pulmonary trunk to the base of the heart. Using retrospective ECG gating, reconstructions were obtained in 10 cardiac phases of the R-R interval.

MDCT Analysis

Digital Imaging and Communications in Medicine data were processed using OsiriX Medical Image Software (version 3.5.1) on an iMac computer (Apple Computer, Cupertino, CA, USA). Multiplanar reformation images were reconstructed at a tim-

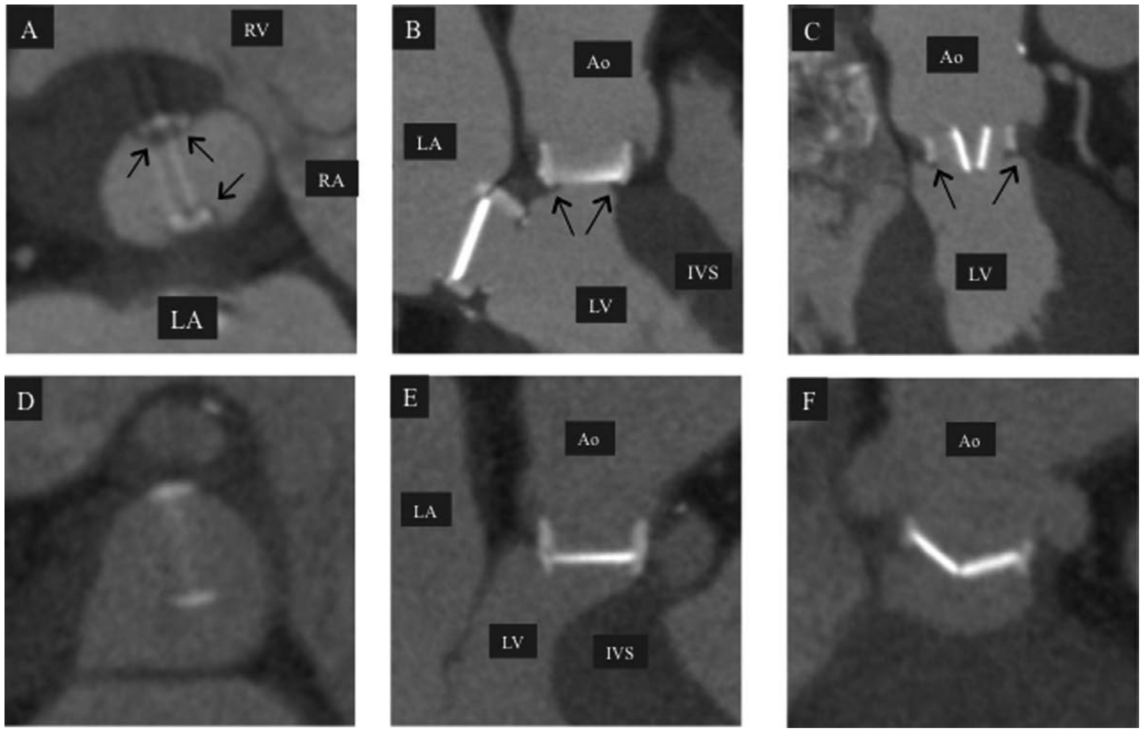

Figure 1. Multidetector-row computed tomography (MDCT) of an aortic prosthetic valve with subprosthetic pannus. (**A**) Short-axis view showing subprosthetic pannus (black arrows) extending from the interventricular septum into the pivot system. (**B**,**C**) Long-axis view parallel and vertical to leaflets showing subprosthetic pannus (black arrows) extending from the interventricular septum into the orifice beyond the prosthetic ring on the ventricular aspect of the prosthetic valve. (**D**–**F**) Normally functioning aortic prosthetic valve showing no periprosthetic overgrown tissue. Ao, aorta; IVS, interventricular septum; LA, left atrium; LV, left ventricle; RA, right atrium; RV, right ventricle.

ing equivalent to 30–40% of the R-R interval (mid-systole) and 60–70% of the R-R interval (diastole). After loading MDCT data, 3 common cardiographic views were created. A short-axis image of the aortic SJM valve was created in a direction similar to that of the surgeon's view. A long-axis view of the left ventricular outflow tract was created in parallel to the axis of the SJM valve leaflets, and the coronal section view was created perpendicular to the left ventricular long-axis view. Multiplanar reconstruction images were independently assessed by 3 experienced observers, including 2 radiologists and 1 cardiac surgeon, who were blinded to this study. In the case of disagreement in evaluation of CT images, final consensus was reached through interobserver discussion. The presence of a periprosthetic abnormality, particularly a sub- or supraprosthetic mass, was assessed initially. If a sub- or supraprosthetic mass was present, the CT attenuation of a sub- or supraprosthetic mass or the interventricular septum was analyzed (ROI=1 mm^2). CT attenuation was measured every 3 points in each target and averaged in each patient. The CT attenuation of the interventricular septum and of any existing periprosthetic abnormalities were measured using every 3 reconstructed images.

Statistical Analysis

Statistical analysis was performed using JMP (version 5.0.1, SAS Institute, Cary, NC, USA) on a Macintosh OS 10.5.8. Data are expressed as mean ± SD. Continuous variables were compared using Student's t-test. Statistical significance was defined as $P<0.001$.

Results

In the 9 patients, VI calculated on echocardiography ranged from 0.27 to 0.48 with a mean of 0.32±0.07. VI was <0.35 in 7 patients, and ≥0.35 in the remaining 2. The opening angle of leaflets observed on cineradiography was ≥20° (range, 23–54°) in all 9 patients (**Table**). No periprosthetic abnormalities, however, were detected on TTE, or on transesophageal echocardiography (TEE). The INR in these 9 patients was 2.03±0.19 (range, 1.75–2.32) at the time of diagnosis of PVO.

MDCT was performed before redo surgery, and the interval between valve implantation and MDCT was 64–260 months with a mean of 128±58.2 months. Heart rate ranged from 52 beats/min to 78 beats/min with a mean of 67 beats/min at the time of MDCT, and adequate images of the left ventricular outflow tract, the SJM valve and the aorta to evaluate periprosthetic abnormality were obtained in all 9 patients. MDCT provided additional findings not detected on TTE or cineradiography. Small subprosthetic masses extending beyond the prosthetic valve ring into the orifice of the valve were detected in all 9 patients (**Figures 1A–C**), and an aneurysm of the sinus of Valsalva was detected in 1. No other abnormalities, however, including valvular masses, supraprosthetic overgrown tissue, abnormal left ventricular outflow tract, and major peri-

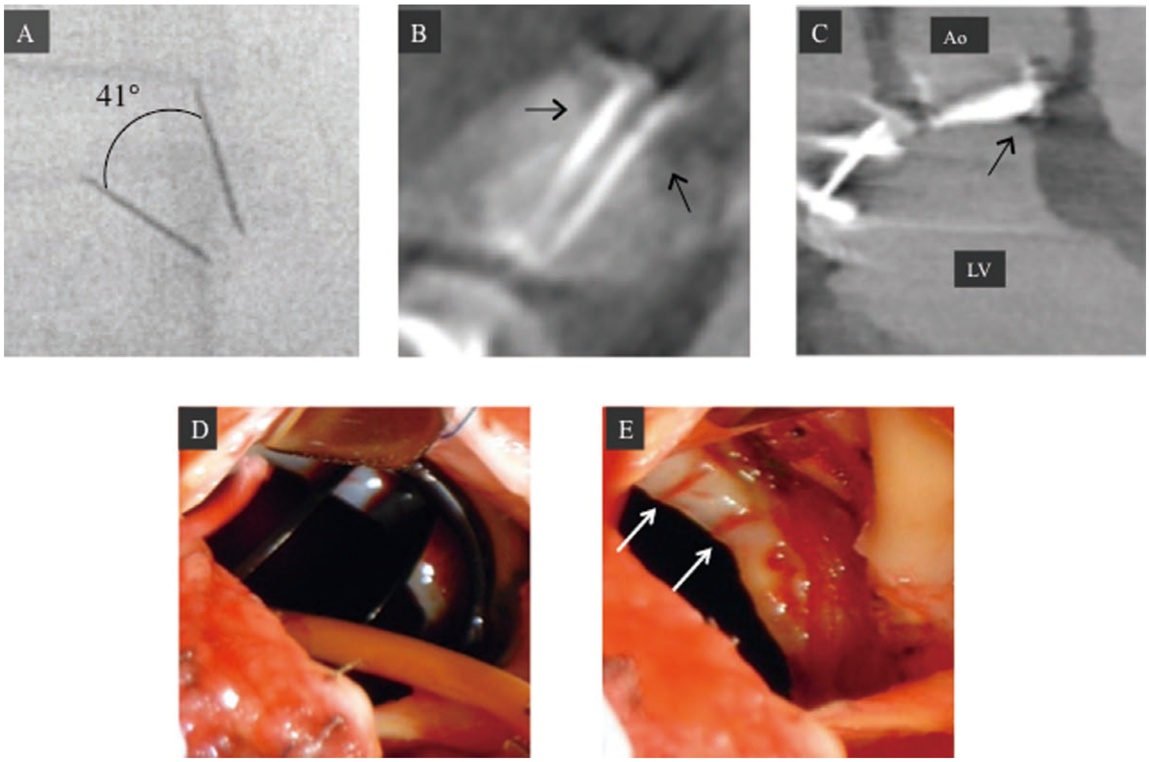

Figure 2. Preoperative cineradiography, multidetector-row computed tomography (MDCT), and operative findings. (**A**) Cineradiography showing restricted opening of the leaflets (41°). (**B**,**C**) Short axis view and long-axis view showing subprosthetic overgrown tissue (black arrows). (**D**) Perioperative photograph (surgeon's view) showing subvalvular pannus invading the pivot guard of the St. Jude Medical valve. (**E**) Perioperative photograph showing 2 fine linear grooves (white arrows) on the subprosthetic overgrown pannus. Ao, aorta; LV, left ventricle.

prosthetic leaks were detected. The most common abnormal finding was subprosthetic mass invading the pivot system of the SJM valve from the interventricular septum on short-axis view of the aortic valve (**Figure 1A**); on left ventricular long-axis view the subprosthetic mass extended from the interventricular septum into the valve orifice beyond the prosthetic ring in the ventricular aspect of the prosthetic valve (**Figures 1B**,**C**). These findings were detected in all 9 patients. In contrast, typical MDCT images in patients with a normally functioning SJM valve without restricted leaflet motion are given in **Figures 1D–F**.

During surgery, a small concentric or eccentric subprosthetic overgrown tissue extending from the interventricular septum into the pivot system in the SJM valve was confirmed in all of the 9 patients (**Figures 2D**,**E**). The subprosthetic overgrown tissue was pathologically diagnosed as pannus.[17] These findings, including the shape, size, and location of the overgrown pannus, corresponded morphologically with the findings observed on MDCT (**Figures 2B**,**C**). Furthermore, 2 fine linear grooves resulting from contact with the 2 leaflet edges were found on the subprosthetic overgrown pannus in all 9 patients (**Figure 2E**). This contact of the leaflet edges with subprosthetic pannus was the cause of restricted leaflet motion in the SJM valves on cineradiogram (**Figure 2A**). No periprosthetic thrombus or valve thrombosis, however, was found in any patient.

CT attenuation of the subprosthetic overgrown pannus in

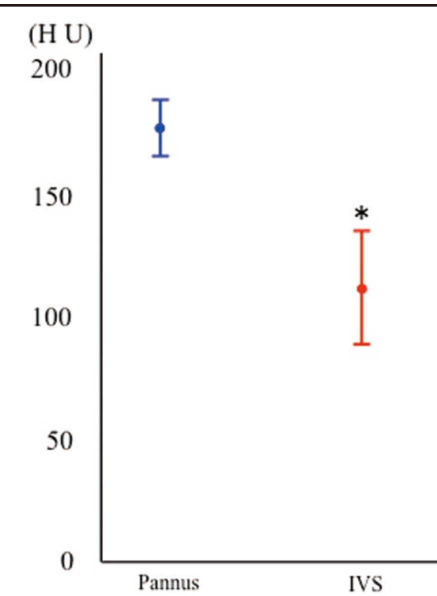

Figure 3. Computed tomography attenuation of pannus ranged from 149 to 189 HU (mean, 170±12 HU) and was significantly different (P<0.0004) from that of the interventricular septum (IVS), which ranged from 77 to 131 HU (mean, 108±24 HU). *P<0.001 vs. pannus.

the 9 patients ranged from 149 HU to 189 HU (mean, 170±12 HU; **Figure 3**). In contrast, mean CT attenuation of the interventricular septum was 108±24 HU (range, 77–103 HU). The mean CT attenuation of the subprosthetic overgrown pannus was significantly greater than that of the interventricular septum (**Figure 3**; P<0.0001).

Discussion

This study has shown that MDCT can be used for clear visualization of the subprosthetic pannus in the aortic position and that identification of the underlying cause of PVO, particularly pannus, can be accomplished by measuring the CT attenuation of periprosthetic masses.

Obstruction of mechanical prosthetic valves due to valve thrombosis or pannus is a serious and occasionally fatal complication. Generally, a major cause of PVO has been thought to be thrombus, and less attention has been given to the role of pannus overgrowth. Rizzoli et al, however, recently found that pannus was the second leading cause of redo operations for mechanical valves in patients with adequate anticoagulation.[5] Echocardiography is the most widely used diagnostic technique to detect malfunctioning prosthetic valves. Cineradiography is also a useful technique for detecting PVO.[2,17,18] Echocardiography provides hemodynamic performance (pressure gradients and valve areas), but artifacts resulting from leaflet movement and lower resolution of the ultrasound image may interfere with detailed observations of the periprosthetic morphology. Although Barbetseas et al indicated that a videointensity ratio of <0.7 on TEE had the best negative predictive value for thrombi on the prosthetic valves,[19] subprosthetic overgrown pannus was not found even on TEE in our experience, because a small amount of pannus or thrombus at the pivot systems generally leads to restricted leaflet motion rather than complete block in the SJM valves.[4,6,12,14] In contrast, cineradiography gives information on leaflet motion in prosthetic valves, but it is not always possible to obtain a tangential view of an implanted bileaflet valve.[11,20] These facts indicate that a combination of echocardiography with cineradiography is the most appropriate for accurate and early diagnosis of PVO.[4,14] An important disadvantage of these techniques, however, is difficulty in visualizing and identifying underlying causes of PVO even by a combination of these 2 techniques. From a surgical standpoint, identification of the exact cause of PVO is essential for deciding the appropriate therapeutic strategy (ie, thrombolysis or surgical treatment).

The role of MDCT in evaluation of prosthetic valve dysfunction has rarely been evaluated in a large number of patients.[18,20–23] In addition to our previous reports of cases,[12–14] the present study has demonstrated that MDCT is a useful and reliable technique for visualizing the subprosthetic abnormality causing PVO and that MDCT can be used to identify the exact cause of PVO by measuring CT attenuation. Symersky et al also evaluated the diagnostic value of MDCT in 13 patients, in whom the cause of PVO was unknown.[18] They found that MDCT imaging provided additional findings not detected on echocardiography or fluoroscopy in 9 of the 13 patients (69%), and that a morphologic substrate for PVO, that is, subprosthetic proliferation of tissue, on MDCT was found in 6 patients. They confirmed MDCT findings by surgery or autopsy in 5 of the 6 patients and they also indicated that the microscopic anatomy of the subprosthetic overgrown tissue consisted of a combination of fibrous tissue and organized thrombus in 3 patients, fibrous tissue in 1, and calcification in 1. Furthermore, Gunduz et al reported a case in which MDCT was useful for definitive diagnosis of mitral prosthetic valve thrombosis and a giant left atrial thrombus, and they concluded that the size and localization of thrombi in the left atrium and on the explanted mechanical mitral valve matched the findings of MDCT.[22]

The CT attenuation for water, air and bone is 0 HU, –1,000 HU, and 1,000 HU, respectively. Measurement of CT attenuation has recently been used to diagnose left atrial thrombus in stroke patients,[23] and other thromboembolic cardiovascular diseases such as prosthetic valve thrombosis, pulmonary embolism and deep vein thrombosis (DVT).[22–26] Symersky et al found no consistent differences in attenuation among different tissues such as fibrous tissue, thrombus, or calcification.[18] Based, however, on the evaluation of the role of MDCT in the management of PVO in 32 patients, Gunduz et al determined that CT attenuation of the abnormal masses adjacent to the prosthetic valve may provide quantitative data for differentiation of pannus from thrombus formation.[24] They reported that the mean CT attenuation of abnormal masses successfully lyzed with thrombolytic therapy was 87 HU (range, 11–180 HU) and that the mean CT attenuation in abnormal masses that did not respond to thrombolytic therapy was 331 HU (range, 168–510 HU). Therefore, they concluded that abnormal masses with HU >200 are usually resistant to thrombolytic therapy. Furthermore, they surgically confirmed that the exact cause of PVO was pure pannus in 6 patients with abnormal masses who did not respond to thrombolytic therapy. Their results imply that periprosthetic pannus, which is resistant to thrombolytic therapy, has a high CT attenuation compared with periprosthetic thrombus. In contrast, in patients with DVT, mean CT attenuation for i.v. thrombi was previously reported to be 31–66 HU,[24–27] and no significant difference was observed between the mean CT attenuation of the pulmonary embolism and that of the DVT clots.[24] Unfortunately, thrombotic obstruction of the prosthetic valve in the aortic position was not found in this patient series, but in our recent study using a 256-slice CT, the mean CT attenuation of a left atrial thrombus and thrombi attached to 2 mechanical prosthetic valves was 85 HU and 90 HU, respectively. Similarly, myxomas in the left atrium had a mean CT attenuation of 41±15 HU. The CT attenuation obtained from subprosthetic pannus in the present patients is not comparable with those obtained from other thromboembolic cardiovascular diseases in previously reported studies[24–27] and in our recent study because CT attenuation varies significantly between different manufacturers' multidetector-row scanners and among different generations of multidetector-row CT scanning equipment.[28] These data, however, suggest the possibility of differentiation between 2 major causes of PVO, pannus and thrombus, by measuring the CT attenuation using MDCT.

Study Limitations

Although the morphologic appearance of subprosthetic pannus on MDCT is considered compatible with intraoperative findings, few data were available on MDCT appearance in a normally functioning prosthetic valve without PVO, as defined on echocardiography and cineradiography. In addition, this study included a small number of patients with PVO, particularly only 9 patients with a subprosthetic overgrown pannus confirmed on MDCT and surgery, because MDCT was not available for the other 21 patients who received replacement of the aortic prosthetic valve for PVO before 2002. Larger series are required to evaluate the role of MDCT in patients with PVO.

Conclusions

The present study has demonstrated that MDCT clearly visualized subprosthetic overgrown pannus in the 9 patients with PVO diagnosed on echocardiography and cineradiography and that the subprosthetic pannus, including the shape, size, and location of the pannus, corresponded morphologically with the findings observed on MDCT. It was also found that the mean CT attenuation of subprosthetic pannus is significantly higher than that of the interventricular septum. This suggests the possibility of differentiation between the 2 major causes of PVO, pannus and thrombus, by measuring CT attenuation of periprosthetic abnormalities.

References

1. Deveri E, Sareli P, Wisenbaugh T, Cronje SL. Obstruction of mechanical heart valve prostheses: Clinical aspects and surgical management. *J Am Coll Cardiol* 1991; **17:** 646–650.
2. Aoyagi S, Fukunaga S, Suzuki S, Nishi Y, Oryoji A, Kosuga K. Obstruction of mechanical valve prostheses: Clinical diagnosis and surgical or non-surgical treatment. *Surg Today* 1996; **26:** 400–406.
3. Vitale N, Renzulli A, Agozzino L, Pollice A, Tedesco N, Schinosa LLT, et al. Obstruction of mechanical mitral prostheses: Analysis of pathologic findings. *Ann Thorac Surg* 1997; **63:** 1101–1106.
4. Aoyagi S, Nishimi M, Kawano H, Tayama E, Fukunaga S, Hayashida N, et al. Obstruction of St. Jude Medical valves in the aortic position: Significance of a combination of cineradiography and echocardiography. *J Thorac Cardiovasc Surg* 2000; **120:** 142–147.
5. Rizzoli G, Guglielmi C, Toscano G, Pistorio V, Vendramin I, Bottio T, et al. Reoperations for acute prosthetic thrombosis and pannus: An assessment of rates, relationship and risk. *Eur J Cardiothorac Surg* 1999; **16:** 74–80.
6. Aoyagi S, Nishimi M, Tayama E, Fukunaga S, Hayashida N, Akashi H, et al. Obstruction of St. Jude Medical valves in the aortic position: A consideration for pathogenic mechanism of prosthetic valve obstruction. *Cardiovasc Surg* 2002; **10:** 339–344.
7. Yamane K, Hirose H, Youdelman BA, Bogar LJ, Diehl JT. Conventional aortic valve replacement for elderly patients in the current era. *Circ J* 2011; **75:** 2692–2698.
8. Padala M, Keeling WB, Guyton RA, Thourani VH. Innovations in therapies for heart valve disease. *Circ J* 2011; **75:** 1028–1041.
9. Sakamoto Y, Hashimoto K, Okuyama H, Ishii S, Shingo T, Kagawa H. Prevalence of pannus formation after aortic valve replacement: Clinical aspects and surgical management. *J Artif Organs* 2006; **9:** 199–202.
10. Tayama E, Aoyagi S. Asymptomatic prosthetic valve dysfunction: Pannus? *Artif Organs* 2002; **26:** 399–401.
11. Aoyagi S, Higa Y, Matsuzoe Y, Nishi Y, Tanaka K, Kawara T, et al. Obstruction of the St. Jude Medical valve: Diagnostic and therapeutic values of cineradiography. *Thorac Cardiovasc Surg* 1993; **41:** 357–363.
12. Teshima H, Hayashida N, Enomoto N, Aoyagi S, Okuda K, Uchida M. Detection of pannus by multidetector-row computed tomography. *Ann Thorac Surg* 2003; **75:** 1631–1633.
13. Teshima H, Hayashida N, Fukunaga S, Tayama E, Kawara T, Aoyagi S, et al. Usefulness of a multidetector-row computed tomography scanner for detecting pannus formation. *Ann Thorac Surg* 2004; **77:** 523–526.
14. Aoyagi S, Fukunaga S, Arinaga K, Shojima T, Ueda T. Prosthetic valve obstruction: Diagnostic usefulness of cineradiography and multidetector-row computed tomography. *Thorac Cardiovasc Surg* 2007; **55:** 515–524.
15. Montorsi P, Cavoretto D, Repossini A, Bartorelli AL, Guazzi MD. Valve design characteristics and cine-fluoroscopic appearance of five currently available bileaflet prosthetic heart valves. *Am J Card Imaging* 1996; **10:** 29–41.
16. Montorsi P, De Bernardi F, Muratori M, Cavoretto D, Pepi M. Role of cine-fluoroscopy, transthoracic, and transesophageal echocardiography in patients with suspected prosthetic heart valve thrombosis. *Am J Cardiol* 2000; **85:** 58–64.
17. Teshima H, Hayashida N, Yano H, Nishimi M, Tayama E, Fukunaga S, et al. Obstruction of St. Jude Medical valves in the aortic position: Histology and immunohistochemistry of pannus. *J Thorac Cardiovasc Surg* 2003; **126:** 401–407.
18. Symersky P, Budde RPJ, de Mol BAJM, Prokop M. Comparison of multidetector-row computed tomography to echocardiography and fluoroscopy for evaluation of patients with mechanical prosthetic valve obstruction. *Am J Cardiol* 2009; **104:** 1128–1134.
19. Barbetseas K, Magiej SF, Pitsavos C, Toutouzas PK, Quinones MA, Zoghbi WA. Differentiating thrombus from pannus formation in obstructed mechanical prosthetic valves: An evaluation of clinical, transthoracic and transesophageal echocardiographic parameters. *J Am Coll Cardiol* 1998; **32:** 1410–1417.
20. Konen E, Gitein O, Feinberg MS, Eshet Y, Raanani E, Rimon U, et al. The role of ECG-gated MDCT in the evaluation of aortic and mitral mechanical valves: Initial experience. *Am J Radiol* 2008; **191:** 26–31.
21. Teshima H, Aoyagi S, Hayashida N, Shojima T, Takagi K, Arinaga K, et al. Dysfunction of an ATS valve in the aortic position: The first reported case caused by pannus formation. *J Artif Organs* 2005; **8:** 270–273.
22. Gunduz S, Ozkan M, Biteker M, Guneysu T. Mechanical mitral valve thrombosis and giant left atrial thrombus: Comparison of transesophageal echocardiography and 64-slice multidetector computed tomography. *Arch Turk Soc Cardiol* 2009; **37:** 483–487.
23. Hur J, Kim YJ, Lee HJ, Ha JW, Heo JH, Choi EY, et al. Left atrial appendage thrombi in stroke patients: Detection with two-phase cardiac CT angiography versus transesophageal echocardiography. *Radiology* 2009; **251:** 683–690.
24. Gunduz S, Duran NE, Biteker M, Guneysu T, Gokdeniz T, Astarcioglu MA, et al. Cardiac 64-slice multidetector computerized tomography in the management of prosthetic heart valve obstruction. *Circulation* 2008; **118:** S1063.
25. Calisir C, Yavas US, Kebapci M, Korkmaz A, Ozkan R. Contribution of the amount of contrast media used in pulmonary CT angiography to assess the diagnostic value of CT venography; comparison of 100 and 150 ml of contrast media. *Clin Radiol* 2009; **64:** 912–917.
26. Cham MD, Yankelevitz DF, Shaham L, Lewis A, Rademaker J, Pearson G, et al. Deep venous thrombosis: Detection by using indirect CT venography. *Radiology* 2000; **216:** 744–751.
27. Loud PA, Katz DS, Klippenstein DL, Shah RD, Grossman ZD. Combined CT venography and pulmonary angiography in suspected thromboembolic disease: Diagnostic accuracy for deep venous evaluation. *AJR Am J Roentgenol* 2000; **174:** 61–65.
28. Bimbaum BA, Hindman N, Lee J, Babb JS. Multi-detector row CT attenuation measurements: Assessment of intra- and interscanner variability with an anthropomorphic body CT phantom. *Radiology* 2007; **242:** 109–119.